Wei Yan*, Weiqing Chen, Xiaobo Zhao, Yindong Yang and Alex McLean

Effect of Cr_2O_3 Pickup on Dissolution of Lime in Converter Slag

DOI 10.1515/htmp-2016-0067
Received March 29, 2016; accepted August 2, 2016

Abstract: Application of low-nickel laterite ore containing chromium as charging material for ironmaking can reduce raw material costs, but result in an increase of chromium content in the hot metal and hence, Cr_2O_3 content in the steelmaking slag, which subsequently causes many problems related to lime dissolution for the steelmaking operation. In this work, a rotating cylinder method was employed to study the effect of Cr_2O_3 on lime dissolution in steelmaking slag. The lime dissolution mechanism, rate control step and affecting factors, including slag basicity, FeO_x and B_2O_3 content, and the formation of phases at reacted layer, were discussed. It was found that mass transfer was the rate control step in slag phase, increase of Cr_2O_3 and slag basicity delayed lime dissolution due to the formation of high-melting temperature phases of $FeO \cdot Cr_2O_3$ spinel and $2CaO \cdot SiO_2$ at the slag/lime reacted interface. Addition of B_2O_3 promoted lime dissolution and suppressed formation of $FeO \cdot Cr_2O_3$ spinel.

Keywords: Cr_2O_3, Lime dissolution, converter slag, low-nickel laterite ore

Introduction

Slagmaking is a key operation in steelmaking, which plays a critical role in dephosphorization reactions during the basic oxygen furnace (BOF) steelmaking. A rapid generation of molten slag during steelmaking can shorten refining time, increase productivity, improve steel quality, reduce production cost and eliminate splashing and sticking lance. High basicity slag containing CaO, MgO, MnO, Fe_xO and SiO_2 is often used in steelmaking process, lime will be added continuously to maintain high slag basicity. An effective steelmaking practice requires rapid dissolution of lime in the early blowing-stage within approximate 4 min to form molten slag for dephosphorization. Therefore, it is important to accelerate lime dissolution during steelmaking. A number of researchers [1–9] have reported their study results on lime dissolution, rate control factors and dissolution mechanism. Typically, Deng et al. [1–3] studied the dissolution of CaO cube in molten converter slags and found that lime dissolution in the slags was very fast in the FeO-SiO_2 slag, and it became slow in the case of FeO-SiO_2-CaO slag. The formation of a dense $2CaO \cdot SiO_2$ layer on the surface of lime particles was the reason to slow down lime dissolution. Hamano et al. [4, 5] studied lime dissolution mechanism and mass transfers between solid lime and molten slag, intermediate phase formation and the rate control step were reported. In addition to these, other researchers [6–9] also reported similar studies.

Similarly, most investigations besides the above only concentrated on lime dissolution in conventional slags without Cr_2O_3. In order to reduce cost of raw materials, a kind of low-nickel laterite ore containing chromium from Indonesia was used as charging material in the blast furnaces in some steel plans in China, and then the hot metal containing chromium was produced for BOF steelmaking. During steelmaking, a significant increase of Cr_2O_3 from zero to almost 8 % as shown in Table 1 was found in the converter slag within 4 min of oxygen blowing according to the sampling analysis, and it caused a series of unexpected problems, such as low lime dissolution rate, low basicity slag, sticky converter slags, high melting temperature, severe lance sticking with the slag, low dephosophorization rate and refining performance. The primary compositions of the ore powders, hot metal and converter slags are listed in Table 1. To the best of our knowledge, very few study on dissolution behavior of lime in Cr_2O_3-containing primary converter slag was reported. Based on the problems found during steelmaking of Cr-containing hot metal, the present study was aimed at covering this gap through investigating the

***Corresponding author: Wei Yan,** State Key Laboratory of Advanced Metallurgy, University of Science and Technology Beijing, Beijing 100083, China; Department of Materials Science and Engineering, University of Toronto, Ontario M5S 3E4, Canada,
E-mail: yanweimetal@gmail.com
Weiqing Chen, Xiaobo Zhao, State Key Laboratory of Advanced Metallurgy, University of Science and Technology Beijing, Beijing 100083, China
Yindong Yang, Alex McLean, Department of Materials Science and Engineering, University of Toronto, Ontario M5S 3E4, Canada

Table 1: Main compositions of ore powders, hot metal and converter slags (in mass percent).

Ore powders	Cr	Ni	P	S	TFe	
	1.725	0.116	0.083	0.072	52.67	
Hot metal	Cr	Si	P	S	Mn	Ti
	0.35	0.46	0.154	0.019	0.59	0.057
Converter slags	CaO/SiO_2	Cr_2O_3	MnO	MgO	Al_2O_3	TFe
4 min slag	0.36	6.81	12.95	1.44	1.53	28.55
Final slag	2.1	2.69	7.32	6.93	2.36	15.57

effect of Cr_2O_3 on the dissolution behavior of lime in primary converter slags by associating the laboratory and industrial studies. Moreover, lime dissolution mechanism, rate control step and affecting factors on lime dissolution in Cr_2O_3-containing primary converter slag were discussed.

Experimental

Experimental materials and slags preparation

Limestone from industrial source was crushed into powder with the size of 200 meshes or less. The powder was mixed with a small amount of water and pressed into cylinders (25 × 25 mm) using a steel model under the pressure of 50 KN. Subsequently, the limestone cylinders were heated in muffle furnace at 1,373 K (1,100 °C) for 3 h to convert limestone to lime. The lime cylinders obtained were placed in a drying box for future lime dissolution tests.

Chemical compositions of experimental slags used to simulate the initial slags of BOF steelmaking were shown in Table 2, which were designed with varying basicity (CaO/SiO_2), Cr_2O_3, and FeO_x and fixed MgO, MnO, Al_2O_3 contents. The slags with the designed compositions were prepared by mixing the reagent grade CaO, SiO_2, Cr_2O_3, MgO, MnO, and Al_2O_3. Before mixture all reagents were dried in advance at 473 K (200 °C) for 3 h to remove moisture. Iron oxide FeO_x powder made from the iron oxide scales of carbon steel rolling were used in the synthetic slags.

Table 2: Chemical compositions of experimental slags (in mass percent).

Slag	CaO/SiO_2	CaO	SiO_2	Cr_2O_3	FeO_x	MgO	MnO	Al_2O_3
L1	0.4	16.0	40.0	0	30	7	6	1
L2	0.4	14.9	37.1	4	30	7	6	1
L3	0.4	13.7	34.3	8	30	7	6	1
L4	0.4	16.6	41.4	8	20	7	6	1
L5	0.4	10.9	27.1	8	40	7	6	1
L6	0.8	21.3	26.7	8	30	7	6	1
L7	1.2	26.2	21.8	8	30	7	6	1

Experimental procedure

Lime dissolution tests were conducted in a high temperature vertical furnace with the rotating cylinder apparatus. The experimental setup is schematically shown in Figure 1. During the experiment, a pure iron crucible (I.D. 46 mm, O.D. 56 mm, height 70 mm) was placed on the alumina base, the position of which was initially adjusted in the constant temperature zone of the furnace. A hole was made in the right of the alumina base for the installation of the thermocouple with the tip in thermal contact with the bottom of the crucible. The diameter, height, and mass of the lime cylinder were measured separately three times, using a digital caliper and balance prior to performing the experiments. The lime cylinder was placed between two thin molybdenum caps, connected using a vertical, rotatable molybdenum shaft of variable speeds, and fixed by a Mo stopper.

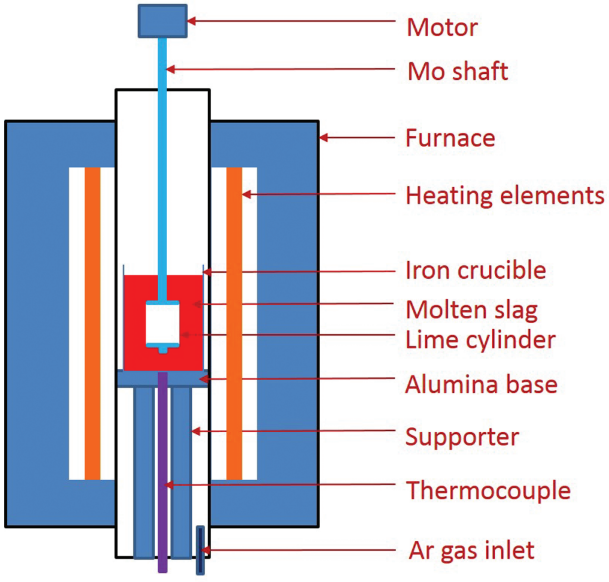

Figure 1: Schematic of experimental apparatus.

Lime dissolution test was carried out when the furnace was heated up to 1,673 K (1,400 °C) and kept constant

under Ar gas atmosphere with a flow rate of 3 L/min. About 180 g slags were added into the crucible through quartz tube. The slags were melted and kept at a constant temperature for 30min for homogenization. Thereafter, the preheated lime cylinder rotating at a speed of 100 rpm was immersed into molten slag at a position of 15mm to the bottom of crucible. After a certain immersion time, the lime cylinder was lifted out quickly from the molten slags for air cooling. After removing the slags adhered to the lime cylinder, the diameter and height of the lime cylinder were measured three times to get a mean value of diameter and height. The white part (unreacted lime) in the core of lime was separated carefully from the black parts (which are reacted lime and penetrated into by the molten slag) with dissecting needle. The mass of the white parts of unreacted lime was weighed. Several black parts in the interfacial region of reacted and unreacted lime were mounted with denture acrylic and polished with alcohol for Scanning Electron Microscopy (SEM) and Energy Dispersive X-ray Spectroscopy (EDS) analysis.

Results

Lime dissolution behavior in the liquid primary converter slags

According to the experimental process, the lime cylinders after cooling are easy to break into small pieces including outside reacted lime (black parts) and inside unreacted lime (inside white parts). Based on this behavior, the lime cylinder after dissolution can be divided into slagging layer (consisting of dissolution layer and reacted layer adhered to the unreacted lime) and unreacted layer from outside to inside along the radius, which are shown schematically in Figure 2. Inevitably, the dissolution and slagging ratios of lime cylinder should be taken into account for quantitative analysis to understand the dissolution process. In this study, lime dissolution is defined as slow and gradual removal or diffusion of CaO from lime into slags. Slagging is defined as penetration degree of slags into lime, which consists of dissolved lime and reacted lime that is still adhering on the surface of lime cylinder.

Lime dissolution rate, R_d (mm/min), defined as decrease in the radius of lime cylinder per unit time, can be calculated using eq. (1).

$$R_d = -\frac{dr}{dt} = -\frac{r - r_0}{t} \tag{1}$$

where r is radius after immersion time t (min), r_0 is original radius of lime cylinder.

The slagging rate of lime, R_s (mm/min), is defined as slagging depth along radius of lime cylinder per unit time, which reveals penetration ability of slag into lime, and can be calculated using eq. (2).

$$R_s = -\frac{dr}{dt} = -\frac{r_u - r_0}{t} \tag{2}$$

The radius r_u of unreacted lime is difficult to measure, which can be calculated indirectly by combining the eqs (3)–(5).

$$V_u = \pi h(r_u^2 - r_i^2) = \frac{W_u}{\rho_{CaO}} \tag{3}$$

$$\rho_{CaO} = \frac{W_0}{V_0} \tag{4}$$

$$r_u = \sqrt{\frac{W_u V_0}{\pi h W_0} + r_i^2} \tag{5}$$

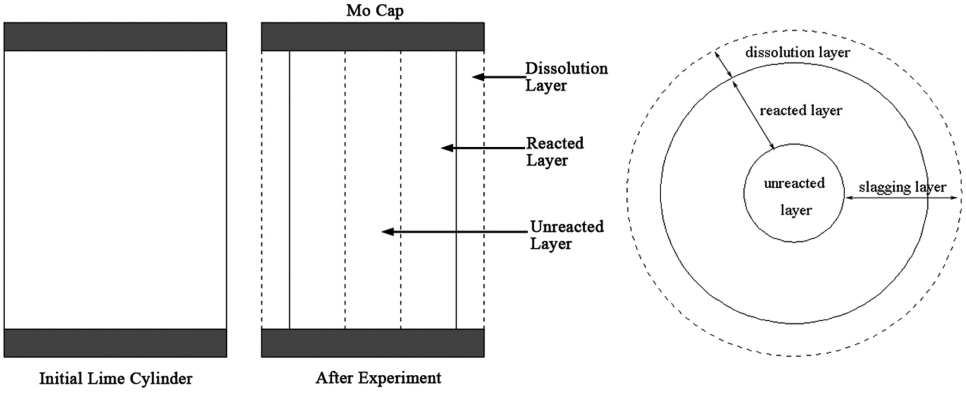

Figure 2: Schematic structure of lime cylinder before and after dissolution.

where r_u is radius of unreacted lime cylinder, V_u and W_u are volume and mass of unreacted lime cylinder. h is height of original lime cylinder, which is considered to be constant. r_i is the radius of inside hole of lime cylinder (3.00 mm) which is designed to fix molybdenum bar of the rotation facility. ρ_{CaO} is density of lime cylinder. W_0 and V_0 are original mass and volume of lime cylinder.

Effect of slag compositions on dissolution rate

Study on dissolution rate of lime in Cr_2O_3 containing converter slags was conducted at a fixed temperature 1,673 K and a revolution speed of 100 rpm. During oxygen blowing for the refining of Cr containing hot metal in converter, the Cr_2O_3 content in the primary slag increased from zero to about 8 % within 4 min according to our field sampling as shown in Table 1. Therefore, study on the influence of Cr_2O_3 on lime dissolution in the converter slag is necessary. Figure 3 illustrates the change of dissolution rate and slagging rate as a function of Cr_2O_3 content in slag with basicity of 0.4 and 30 % FeO_x. It can be seen that dissolution and slagging rate of lime decrease obviously with increasing Cr_2O_3 content. The slagging rate (including dissolution and slag penetration) is far more than dissolution rate, which indicates the slag penetration is typically faster than dissolution. But slagging rate decreases obviously which indicates Cr_2O_3 inhibits the penetration of slag into lime. Very few study on effect mechanism of Cr_2O_3 on lime dissolution and slag penetration has been reported in publications, which will be discussed below.

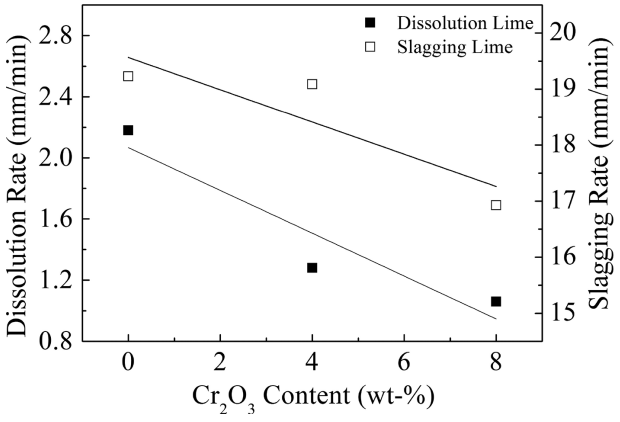

Figure 3: Effect of Cr_2O_3 on lime dissolution and slagging rate.

The influence of basicity (CaO/SiO_2 mass ratio) of primary slags on the dissolution and slagging rate of lime cylinder in the converter slag with 8 % Cr_2O_3 were examined, the results obtained are presented in Figure 4. It can be observed that lime dissolution and slagging rate decrease with increasing basicity. Figure 5 shows the effect of FeO_x on dissolution and slagging rate of lime in converter slag with basicity of 0.4 and 8 % Cr_2O_3. It was seen that the addition of FeO_x significantly increases the dissolution and slagging rate.

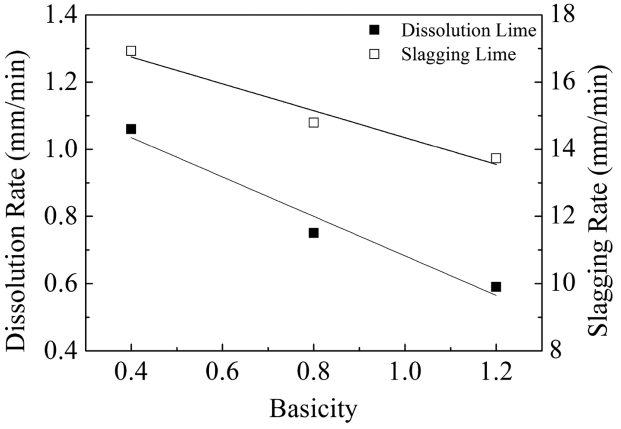

Figure 4: Effect of basicity on lime dissolution and slagging rates.

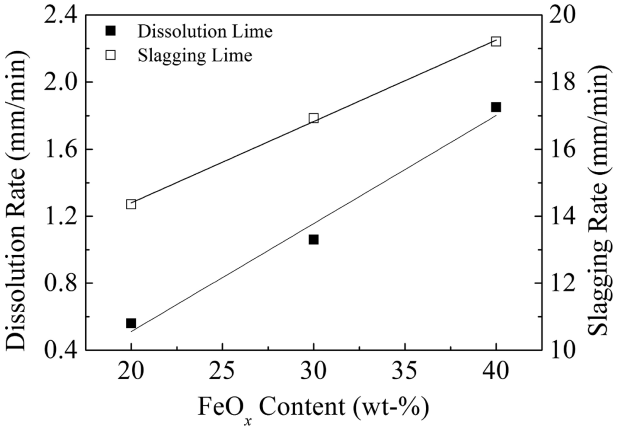

Figure 5: Effect of FeO_x content on lime dissolution and slagging rate.

Discussion

Rate control step of lime dissolution

The effect of revolution speed on lime dissolution in Cr_2O_3 containing slags was examined using slag L3 with basicity of 0.4 and 8 % Cr_2O_3. The revolution speed during the test was in the range of 100–300 rpm. Figure 6 illustrates the

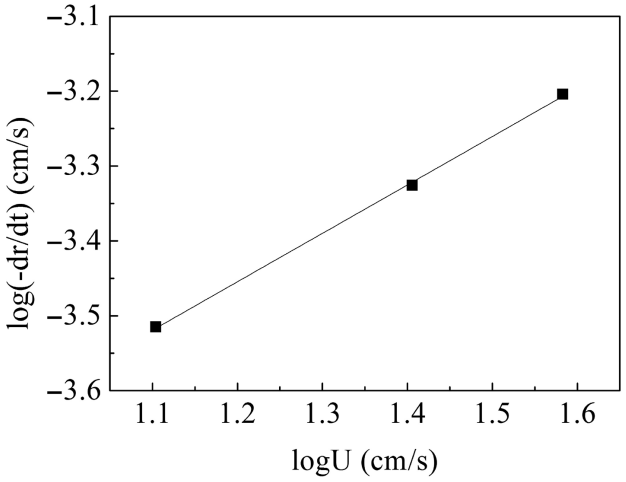

Figure 6: Relationship between lime dissolution rate and revolution speed.

relationship between logarithms of lime dissolution rate, R_d (cm/s), and logarithms of periphery velocity U (cm/s) of rotating lime cylinder, which can be calculated according to the eq. (6) [10].

$$R_d = -\frac{dr}{dt} = A \cdot U^b \tag{6}$$

Periphery velocity U can be calculated using eq. (7).

$$U = \frac{\pi \bar{d} m}{60} \tag{7}$$

where A is constant, U is periphery velocity (cm/s), $\bar{d}$ is mean diameter (mm) of lime cylinder, m is revolution speed of lime cylinder (rpm), b can be obtained by regression using the experimental data. Previous studies reported that b value was 0.48, 0.57, or 0.69, for dissolution of lime [10–12], and 0.88 or 0.81 for dolomite and alumina [13, 14], respectively.

It can be seen from Figure 6 that $\log R_d$ (cm/s) increases linearly with increasing $\log U$ (cm/s), which means that increasing revolution speed can accelerate dissolution of lime in Cr_2O_3 containing converter slags. As shown in Figure 6, the b value of 0.7 can be obtained by calculating the slope of the line presented in Figure 6, which is close to the values reported in references [10–12]. From the aforementioned result it can be reasonably concluded that the lime dissolution rate in Cr_2O_3 containing converter slag mainly depends on the rotation speed, and hence mass transfer across the boundary layer can be the rate control step of lime dissolution under the present experimental conditions.

The mass transfer flux J (g/cm^2 · min) of lime can be expressed as eq. (8).

$$J = k(n_i - n_b) \tag{8}$$

where k is mass transfer coefficient of lime in the converter slag, (cm/min). n_i and n_b are mass densities of lime at the lime/slag interface and in the liquid bulk slag, respectively, (g/cm^3).

The relationship between mass transfer flux J and dissolution rate $-dr/dt$ can be obtained by the mass balance equation expressed as eq. (9).

$$\rho_{CaO} \cdot A \cdot \left(-\frac{dr}{dt}\right) = A \cdot J \tag{9}$$

where ρ_{CaO} is the density of lime cylinder (g/cm^3). A is interfacial area between lime cylinder and liquid converter slag (cm^2).

Combining eqs (8) and (9), lime dissolution rate can be derived and written as eq. (10).

$$R_d = -\frac{dr}{dt} = \frac{k\rho_b}{100\rho_{CaO}} \cdot \Delta(\%CaO) \tag{10}$$

where ρ_b is the density of converter slag (g/cm^3). Δ(%CaO) (mass percent) is assumed to be equal to the concentration difference between saturation and initial concentration of CaO in the liquid bulk slag. Lime saturated concentration in the molten slag can be determined from the liquids line on the pseudo "CaO"-SiO_2-"FeO_x" ternary phase diagram using FactSage 6.2 software.

Since Mo caps were used to cover the top and bottom surfaces of lime cylinder, and only the cylinder side was in contact with converter slag, the dissolution of the side surface of the lime cylinder should represent dissolution pattern. Kosaka [15] derived the eq. (11) to describe the dependence of mass transfer coefficient k on Reynolds number Re, Schmidt number Sc and periphery velocity U (cm/s). Here $Re = (\rho_b U d)/\eta$, $Sc = \eta/(\rho_b D)$, $U = \omega r$. The diffusion coefficient D of lime is associated with the slag properties by Stokes-Einstein equation (12) [16]. Obviously, these parameters are related to physical properties of liquid converter slag (density $_b$, dynamic viscosity of converter slags) and angular velocity of lime cylinder.

$$k = 0.065 \cdot Re^{-1/4} \cdot Sc^{-2/3} \cdot V \tag{11}$$

$$D = \frac{k_B \mathrm{T}}{6\pi r \eta} \tag{12}$$

where k_B is the Boltzmann constant, T is the Kelvin temperature, r is the effective molecules radius.

Combining eqs (10) through (12), lime dissolution rate, $-dr/dt$ (cm/min), can be derived and written as eq. (13).

$$R_d = -\frac{dr}{dt} = \frac{\Delta(\%CaO)\rho_b}{100\rho_{CaO}} \cdot 0.065 \cdot \mathrm{Re}^{-1/4} \cdot Sc^{-2/3}.$$
$$U = \frac{0.055}{100\rho_{CaO}} \left(\frac{k_B T}{6\pi r}\right)^{2/3} \omega^{3/4} \rho_b^{17/12} \eta^{-13/12} \Delta(\%CaO) \quad (13)$$

Assuming that ρ_{CaO} is constant, eq. (13) can be grouped into three parts: (1) A constant part $\frac{0.055}{100\rho_{CaO}} \left(\frac{k_B T}{6\pi r}\right)^{2/3}$ which is independent on slag composition; (2) second part is $^{3/4}$which is related to experimental conditions; and (3) third part is $\rho_b^{17/12} \eta^{-13/12} \Delta(\%CaO)$ which depends on converter slag compositions. For the same converter slag, $\frac{0.055}{100\rho_{CaO}} \left(\frac{k_B T}{6\pi r}\right)^{2/3}$ and $\rho_b^{17/12} \eta^{-13/12} \Delta(\%CaO)$ can be viewed as constants due to minimal dissolution of lime into massive slag (180 g). Therefore, lime dissolution rate should be proportional exponentially to revolution speed of lime cylinder to the power of 0.75, which is very close to the power of 0.7 obtained in the present study and falls well in the range of 2/3 to 4/5 reported in the reference [17]. This implies that mass transfer across boundary layer is the rate control step for lime dissolution into Cr_2O_3 containing slags with a fixed compositions.

Effect of slag compositions

According to eq. (13), the effect of varying converter slags on lime dissolution rate in molten slags is mainly determined by the third part of the eq. (13), that is $\rho_b^{17/12} \eta^{-5/12} \Delta(\%CaO)$. In the present study, Mills's density model [18] of slags is employed to estimate the density of Cr_2O_3 containing converter slags. The calculated value of the slag density is about 3.3g/cm^3, which can be assumed as a constant compared to other parameters because the change of the density value is very small.

Models are not available for the calculation of the viscosity of Cr_2O_3 containing slags. However the works reported by Tunezo [19, 20] showed that addition of Cr_2O_3 could increase slag viscosity for CaO-SiO_2-Cr_2O_3 and CaO-SiO_2-Cr_2O_3-FeO systems; while increase of slag basicity and FeO_x content would reduce slag viscosity. The relationship between viscosity and diffusion in molten slag were usually described in Eyring relation and Stokes-Einstein relation. Eyring's studies [16, 21] reported an inversely proportional relationship between lime diffusivity D in liquid slags and viscosity of liquid slags. The finding in this work agrees well with the relationship suggested by Eyring et al. that increasing viscosity inhibits CaO diffusion across boundary layer. That means addition of Cr_2O_3 inhibits lime diffusion but increases of basicity and FeO_x promotes lime diffusion.

However, it was found that dissolution rate of lime decreased with increasing basicity. This could be due to the reason that an increase of basicity would result in an increase of lime concentration in the molten slag, and hence a decrease of driving force of lime diffusion as shown in Figure 7. Therefore, basicity influences lime dissolution mainly through decreasing driving force. Nevertheless, increases in Cr_2O_3 and FeO_x only introduce a negligible effect on driving force. So driving force is not the main influence aspect on dissolution in slag with varying Cr_2O_3 and FeO_x contents. Apart from this, slag compositions will affect lime dissolution by changing phases formed in the lime/slag reacted interface, which will be discussed in the following section.

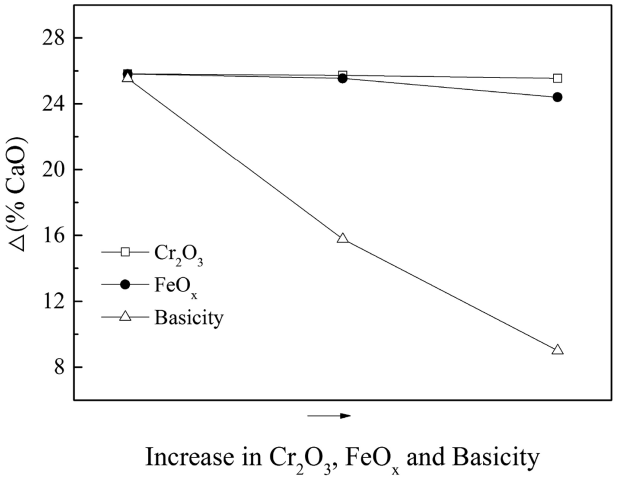

Figure 7: Effect of Cr_2O_3, FeO_x and basicity on driving force.

Effect mechanism of Cr_2O_3 on lime dissolution

The above discussion focuses on the effect of liquid slag properties on diffusion of CaO across boundary layer. However, undissolvable solid layer or intermediate phases formed in the lime/slag interface can also lead to a significant effect on lime dissolution in CaO-FeO-SiO_2 slags [1–5, 14]. To the best of our knowledge, effect of Cr_2O_3 in molten slag on the formation of intermediate phase in the boundary of the solid lime and molten slag has not been reported, and hence it is extremely necessary to make this mechanism clear. Figure 8 shows SEM image of slag sample taken from the lime dissolution in molten slag L2 ($CaO/SiO_2 = 0.4$, 4 %Cr_2O_3). A high concentration for Si, Ca,

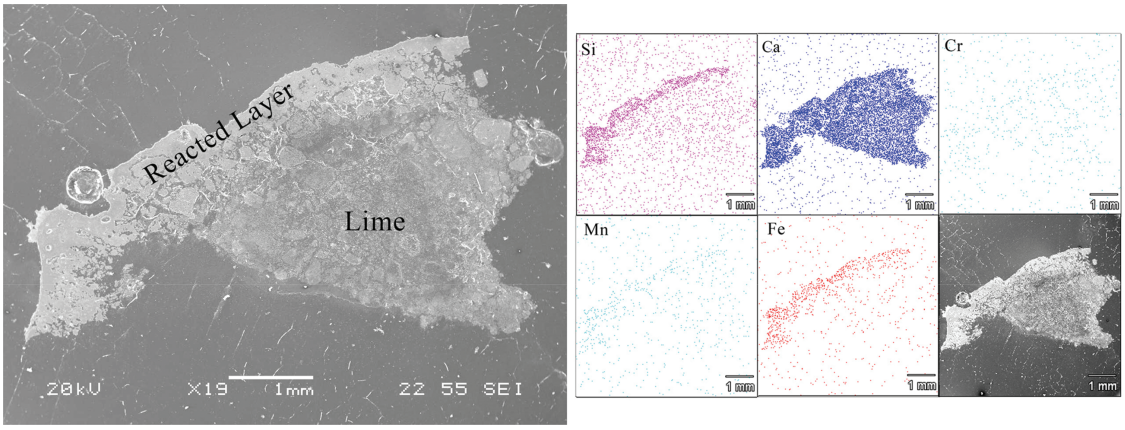

Figure 8: SEM and element distributions in slag/lime interface after lime dissolution in slag L2 (4 % Cr_2O_3).

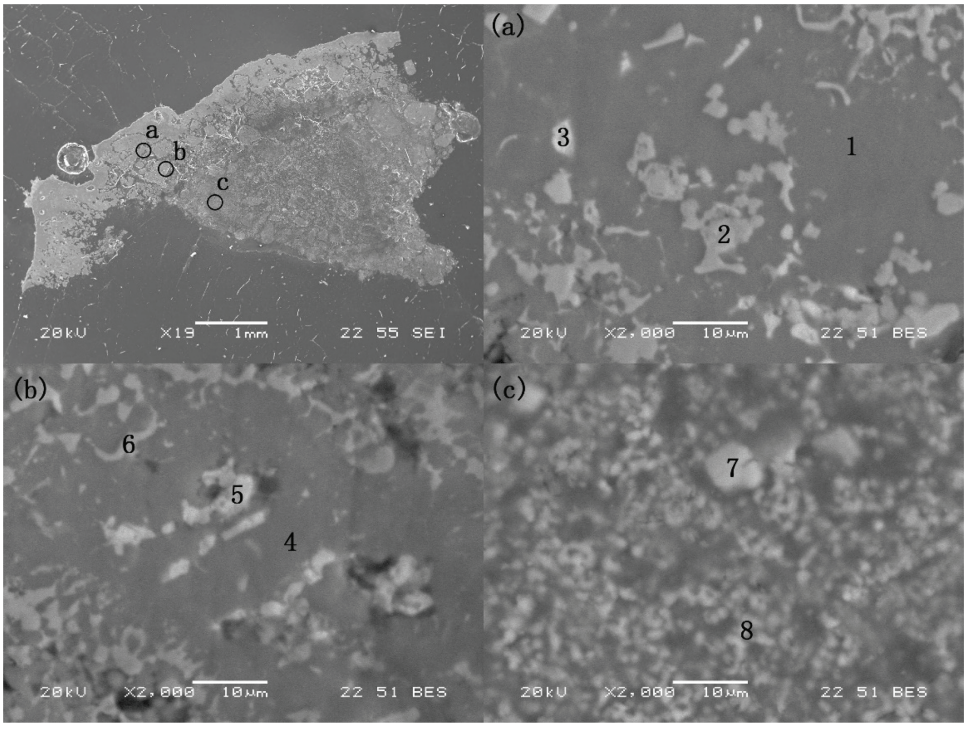

Figure 9: Phase morphology and compositions from reacted layer after lime dissolution in slag L2 (4 % Cr_2O_3), (a) outer layer, (b) middle layer and (c) inner layer, phases 1–8 are listed in Table 3.

Cr or Fe can be found in the surface region of lime cylinder contacted with molten slag. Figure 9 presents the SEM images obtained in the slag/lime interface including: (a) outer layer near the slag, (b) middle layer and (c) inner layer near the unreacted lime. In the out layer of the slag, more $2CaO \cdot SiO_2$ and $FeO \cdot Cr_2O_3$ phases can be found (see Figure 9(a)). In the middle layer, $2CaO \cdot SiO_2$ seems to decrease and some $3CaO \cdot SiO_2$ and $CaO \cdot MgO \cdot SiO_2$ phases are found (see Figure 9(b)). In the inner layer, the majority of the phases is unreacted lime (see Figure 9(a)). It is well known that $2CaO \cdot SiO_2$ is the primary phase with high melting temperature, which can slow down CaO diffusion across the interface according to the previous studies [2, 14]. However, the important finding in the current study is that a large quantity of $FeO \cdot Cr_2O_3$ spinel is formed in the reacted interface region. $FeO \cdot Cr_2O_3$ spinel has high

melting temperature (2,373 K (2,100 °C)) which is similar to the melting temperature (2,403 K (2,130 °C)) of $2CaO \cdot SiO_2$ [22]. Penetration of FeO_x breaks the $2CaO \cdot SiO_2$ layer but on the other hand FeO_x participates in the formation of $FeO \cdot Cr_2O_3$ spinel. These high melting temperature phase $FeO \cdot Cr_2O_3$ was distributed in the discontinuous $2CaO \cdot SiO_2$ and mixed with them. Consequently, the formation of $FeO \cdot Cr_2O_3$ spinel will play the similar role as $2CaO \cdot SiO_2$ to inhibit lime dissolution together with $2CaO \cdot SiO_2$. With further increase of Cr_2O_3 in the test slag L3($CaO/SiO_2 = 0.4$, 8 %Cr_2O_3), more $FeO \cdot Cr_2O_3$ spinel are found in slag/lime interface as shown in Figure 10, which will further slow-down lime dissolution.

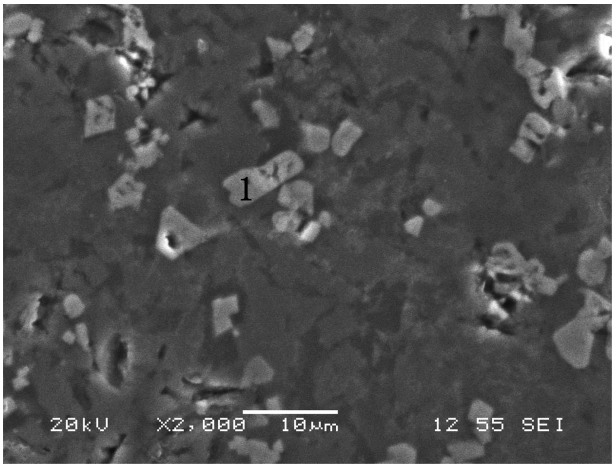

Figure 10: Phase morphology and compositions in the slag/lime reacted interface after dissolution in slag L3 (8 % Cr_2O_3), phase 1 is listed in Table 3.

The above analysis reveals that during lime dissolution in the conventional CaO-FeO-SiO_2 converter slag, $2CaO \cdot SiO_2$ phase can form on the surface of lime particles and it inhibits lime dissolution. Addition of Cr_2O_3 in the molten slag promotes the formation of $FeO \cdot Cr_2O_3$ spinel with high melting temperature and slows down lime dissolution. Meanwhile, an increase of FeO_x in molten slag still accelerated lime dissolution but addition of Cr_2O_3 also weaken the positive effect of FeO_x on lime dissolution due to formation of $FeO \cdot Cr_2O_3$ spinel. Therefore, what is the different from the common Cr_2O_3-free CaO-FeO-SiO_2 slag is FeO_x is not the optimal option to promote lime dissolution due to its participation into the formation of $FeO \cdot Cr_2O_3$ spinel. An additive which promotes lime dissolution by inhibiting the formation of $FeO \cdot Cr_2O_3$ spinel should be considered.

Effect and mechanism of B_2O_3 on lime dissolution in Cr_2O_3-containing slag

Based on the above analysis and consideration on potential application of low-cost and abundant paigeite in China, 0–4 % B_2O_3 was firstly tried to be added into 8 % Cr_2O_3-containing converter slag(master slag L3) to experimentally investigate its effect on lime dissolution. The observed effect of B_2O_3 on dissolution rate was shown in Figure 11. It can be seen the dissolution rate increases with the addition of B_2O_3 from 0 to 4 %. On the one hand, addition of B_2O_3 will decrease the slag viscosity which benefits for the diffusion of lime into slag according to eqs (12) and (13). On the other hand, it also can be seen from SEM image of slag/lime reacted interface shown in Figure 12 and Table 4 addition of 4 %B_2O_3 suppresses the precipitation of $FeO \cdot Cr_2O_3$ spinel. No $FeO \cdot Cr_2O_3$ can be found in the SEM analysis of reaction layer of lime and slag (master slag L3 + 4 %B_2O_3). It can be that concluded B_2O_3 promotes lime dissolution by combination of decreasing viscosity and suppressing formation of $FeO \cdot Cr_2O_3$ spinel.

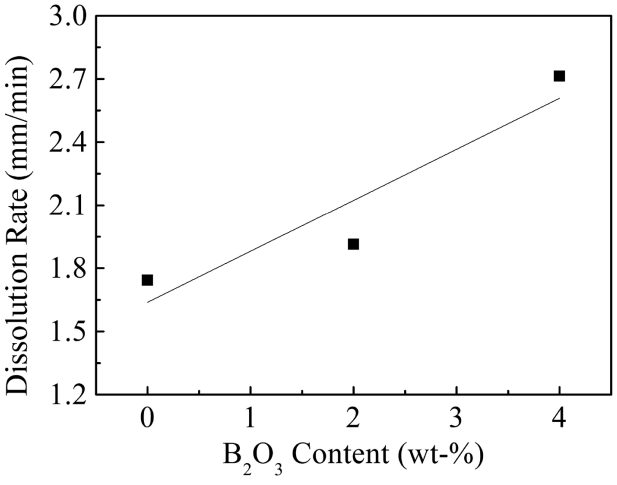

Figure 11: Effect of B_2O_3 on lime dissolution rate.

Consideration on solutions to the problems

As mentioned above, the low dephosphorization, sticking lance, bad flow ability and high melting temperature of converter slag can be contributed to poor lime dissolution and excess increase of Cr_2O_3 in slag during the blowing period. Meanwhile, increase of Cr_2O_3 also restricted the lime dissolution. These poor BOF performance instead may increase the cost. Based on these

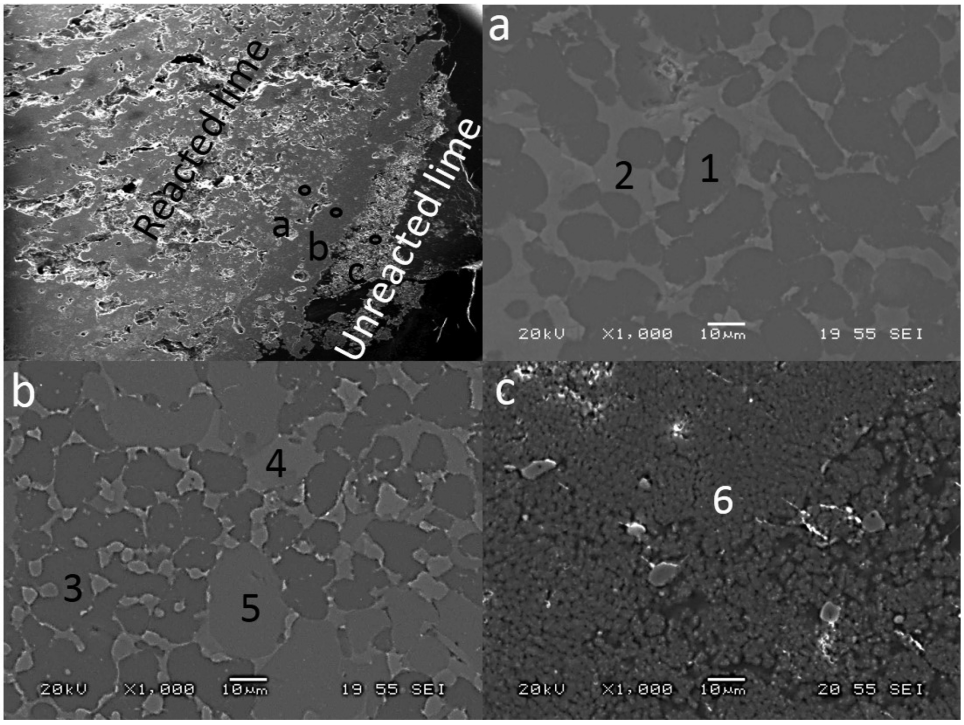

Figure 12: Phase morphology and compositions from reacted layer after lime dissolution in slag L2. (8 % Cr_2O_3 + 4 % B_2O_3), (a) outer layer, (b) middle layer and (c) inner layer, phases 1–6 are listed in Table 4.

Table 3: Phase and their chemical compositions in the vicinity of slag/lime interface.

Samples (Figures)	Label	Primary phase	Chemical compositions of phases						
			CaO	SiO_2	Cr_2O_3	FeO	MgO	MnO	Al_2O_3
L2 (Figure 9)	1	$2CaO \cdot SiO_2$	56.88	34.15	0	4.48	4.49	0	0
	2	$FeO \cdot Cr_2O_3$	4.05	1.68	12.02	64.21	6.17	8.8	3.06
	3	$3CaO \cdot SiO_2$	75.3	17.44	0	4.37	2.89	0	0
	4	$2CaO \cdot SiO_2$	56.32	34.79	0	3.35	5.54	0	0
	5	$3CaO \cdot SiO_2$	80.57	12.38	0	7.05	0	0	0
	6	$CaO \cdot MgO \cdot SiO_2$	32.11	17.79	0	6.35	25.31	17.5	0.95
	7	$2CaO \cdot SiO_2$	66.69	28.5	0	0	0	0	4.82
	8	CaO	100	0	0	0	0	0	0
L3 (Figure 10)	1	$FeO \cdot Cr_2O_3$	1.91	2.67	38.43	54.51	2.48	0	0

analyses, some initial measures can be taken from the technical and economic perspectives to alleviate these issues for achieving application of low-cost laterite and meanwhile good BOF performance as far as possible, such as increasing the activity of lime to promote its dissolution in early blowing, reducing the addition of laterite to restrict Cr content to less than 0.5-wt % in hot metal, adding some bauxite to decrease melting temperature, adjusting the lance height to change the FeO content in slag. The above measures have been taken and achieved positive effect. Effectiveness of paigeite addition in alleviating these problems is expected to be examined next during BOF process to achieve more utilization of low-cost laterite.

Table 4: Phase and their chemical compositions in the vicinity of slag/lime interface.

Samples (Figures)	Label	Primary phase	Chemical compositions of phases						
			CaO	SiO_2	Cr_2O_3	FeO	MgO	MnO	Al_2O_3
L3 + 4 %B_2O_3 (Figure 12)	1	$2CaO \cdot SiO_2$	67.71	30.22	0	2.08	0	0	0
	2	$CaO \cdot FeO$	45.99	1.46	1.56	48.50	0	0	2.49
	3	$3CaO \cdot SiO_2$	71.43	28.57	0	0	0	0	0
	4	$CaO \cdot FeO$	48.63	0	0	48.29	0	0	3.08
	5	CaO	84.9	0	0	8.67	1.45	4.98	0
	6	CaO	98.85	0	0	0	1.15	0	0

Conclusions

Lime dissolution behavior and dissolution mechanism in Cr_2O_3-containing converter slags were studied by rotating cylinder method at 1,673K (1,400 °C), the phases formed in the slag/lime reacted interface were examined using SEM/EDS analysis. The results obtained are summarized as follows:

1. Lime dissolution and slagging rate decreased with increasing Cr_2O_3 content and slag basicity, but increased with increasing FeO_x content in Cr_2O_3-containing converter slag.
2. A linear relationship between logarithms of lime dissolution rate and revolution speed of the lime cylinder was found and it demonstrated that mass transfer is the rate control step in slag phase for lime dissolution in Cr_2O_3-containing slag.
3. Addition of Cr_2O_3 into the converter slag promoted the formation of high melting temperature phase $FeO \cdot Cr_2O_3$ in the lime/slag reacted interface and slowed down lime dissolution in the Cr_2O_3-containing converter slag. Addition of FeO_x promoted lime dissolution but also participated in formation of $FeO \cdot Cr_2O_3$ spinel. Addition of B_2O_3 into Cr_2O_3-containing converter slag promoted the lime dissolution and meanwhile suppressed formation of $FeO \cdot Cr_2O_3$ spinel.
4. Measures such as improving lime property, adjusting BOF operation and adding low-cost fluxing agent were tried and suggested to alleviate the issues and achieve more utilization of low-cost laterite ore.

References

[1] T.F. Deng and S.C. Du, Metall. Mater. Trans. B, 43 (2012) 578–586.
[2] T.F. Deng, J. Gran and S.C. Du, Steel Research Int., 81 (2010) 347–355.
[3] T.F. Deng, B. Glaser and S.C. Du, Steel Research Int., 83 (2012) 259–268.
[4] T. Hamano, M. Horibe and K. Ito, ISIJ Int., 44 (2004) 263–267.
[5] T. Hamano, S. Fukagai and F. Tsukihash, ISIJ Int., 46 (2006) 490–495.
[6] S.H. Amini, M.P. Brungs, S. Jahanshahi and O. Ostrovski, Metall. Mater. Trans. B, 37 (2006) 773–780.
[7] S. Amini, M. Brungs and O. Ostrovski, ISIJ Int., 47 (2007) 32–37.
[8] J. Yang, M. Kuwabara, T. Asano, A. Chuma and J. Du, ISIJ Int., 47 (2007) 1401–1408.
[9] Z.S. Li, M. Whitwood, S. Millman and J. Boggelen, Ironmaking Steelmaking, 41 (2014) 112–120.
[10] M. Matsushima, S. Yadoomaru, K. Mori and Y. Kawai, Trans. ISIJ, 17 (1977) 442–449.
[11] N. Maruoka, A. Ishikawa, H. Shibata and S.Y. Kitamura, High Temp. Mater. Process., 32 (2013) 15–24.
[12] R. Tang, Y. Wang, C.J. Zhang, B. Xie and J. Diao, Ironmaking Steelmaking, 42 (2014) 169–175.
[13] M. Umakoshi, K. Mori and Y. Kawai, Trans. ISIJ, 24 (1984) 532–539.
[14] S. Taira, K. Nakashima and K. Mori, ISIJ Int., 33 (1993) 116–123.
[15] M. Kosaka and S. Minowa, Tetsu to Hagane, 52 (1966) 1748–1762.
[16] H.A. Kooijman, Ind. Eng. Chem. Res., 41 (2002) 3326–3328.
[17] K. Hirota, Kinetics of Reaction, Kyoritsu Shuppan Press, Tokyo (1964).
[18] K.C. Mills, Y. Lang and R.T. Jones, J. S. Afr. I. Min. Metall., 11 (2011) 649–658.
[19] S. Tunezo and S. Keizo, Tetsu to Hagane, 51 (1965) 1851–1854.
[20] S. Tunezo and S. Keizo, Tetsu to Hagane, 51 (1965) 1855–1857.
[21] S. Glasstone, K.J. Laidlev and H. Eyring, The Theory of Rate Processes: The Kinetics of Chemical Reactions, Viscosity, Diffusion and Electrochemical Phenomena, McGraw-Hill, New York (1941).
[22] V.D. Eisenhüttenleute, Slag Atlas (2nd edition), Verlag Stahleisen GmbH, Düsseldorf (1995).